applied sciences

MDPI

Article

# Application of Adaptive Neuro-Fuzzy Inference Systems with Principal Component Analysis Model for the Forecasting of Carbonation Depth of Reinforced Concrete Structures

**Juan Liu** [1] **and Xuewei Bai** [2,*]

[1] School of Civil Engineering, Liaoning Petrochemical University, Fushun 113001, China; liujuan@lnpu.edu.cn
[2] College of Engineering, Shenyang Agricultural University, Shenyang 110866, China
* Correspondence: bai-xuewei@syau.edu.cn; Tel.: +86-139-4011-2365

**Abstract:** The carbonation of reinforced concrete is one of the intrinsic factors that cause a significant decrease in service performance in concrete structures. To decrease the effect of carbonation-induced corrosion during the lifetime of the concrete structure, a prediction of carbonation depth should be made. The carbonation of concrete is affected by many factors, such as the compressive strength of the concrete, service life, carbonation time, carbon dioxide concentration, working stress, temperature, and humidity. On the basis of these seven parameters, combined with the predictive power of the adaptive network-based fuzzy inference system (ANFIS) and principal component analysis (PCA), which can reduce data dimensions before modeling, we introduced a novel approach—the PCA–ANFIS model—that can predict the carbonation of reinforced concrete. Practical engineering examples were adopted to verify the superiority of the suggested PCA–ANFIS model, with 90% of the carbonation depth data used for training and 10% used for testing. The root mean square error (RMSE) values for the ANFIS, ANN, PCA–ANN, and PCA–ANFIS training were 12.23, 6.28, 5.42, and 1.38, respectively. The results showed that the PCA–ANFIS model is accurate and can be used as a fundamental tool for predicting the service life of concrete structures.

**Keywords:** carbonation depth of reinforced concrete structures; principal component analysis (PCA); adaptive network-based fuzzy inference system (ANFIS); forecast



**Citation:** Liu, J.; Bai, X. Application of Adaptive Neuro-Fuzzy Inference Systems with Principal Component Analysis Model for the Forecasting of Carbonation Depth of Reinforced Concrete Structures. *Appl. Sci.* **2023**, *13*, 5824. https://doi.org/10.3390/app13105824

Academic Editors: Chia-Ming Fan, Po-Wei Li and Jakub Krzysztof Grabski

Received: 7 April 2023
Revised: 5 May 2023
Accepted: 7 May 2023
Published: 9 May 2023



## 1. Introduction

Concrete is one of the most widely used and versatile building materials in the world. However, the carbonation of concrete poses a significant threat to its structural integrity. This process occurs when the alkali in the concrete structure reacts with carbon dioxide ($CO_2$) in the environment, resulting in the production of calcium carbonate ($CaCO_3$). As a result, the basicity of the concrete environment is reduced, and its original protective effect for reinforcement is compromised. This is the primary reason for steel bar corrosion in concrete [1]. In reinforced concrete structures, corrosion of the reinforcement can cause the corroded products to expand, generating pressure on the surrounding concrete. This pressure can eventually lead to the deterioration of the concrete's durability. Thus, understanding the carbonation process and its impact on concrete structures is crucial for ensuring their longevity and safe use.

Concrete carbonation is a complex physicochemical process involving numerous unknown factors. Due to the random nature of building environments and the uncertainties regarding concrete quality, carbonation depth in concrete structures is highly variable and difficult to predict. Even in identical environmental conditions, carbonation depth can be vastly different for concrete structures of the same strength [1]. As a result, understanding the underlying mechanisms of carbonation and its impact on concrete structures is critical to ensuring the longevity and safety of these structures.

Carbonation modeling and the prediction of carbonation depth are essential for evaluating the durability of reinforced concrete structures [2]. Over the past few decades, numerous experts and scholars have analyzed concrete carbonation theory and experimentation in order to develop prediction models. Niu Ditao et al. developed a calculation model for predicting carbonation depth based on carbonation theory and experimental results [3], while Khunthongkeaw et al. proposed a mathematical approach to predict carbonation depth based on accelerated tests [4]. However, it is important to consider environmental conditions as influencing factors in carbonation rates. Yamada et al. evaluated the influence of environmental conditions on the carbonation process in concrete structures, while Woyciechowski et al. presented the "self-terminated carbonation model," which takes into account these factors [5,6].

Wu et al. [7] established predictive modeling for the depth of carbonation of iron tailings powder concrete by introducing various influential factors. The carbonation process is very complex and is influenced by many factors, and there is interaction between biochemical factors, such as fungi and mildew; these factors affect the carbonation reaction. Modern machine learning algorithms can construct forecasting models with effects from empirical data, which may then be used to forecast features in future investigations [8].

Given that the carbonation process is complex and influenced by multiple factors, including interactions with biochemical factors such as fungi and mildew, artificial intelligence can provide new research avenues for carbonation depth forecasting. Neural network models, such as the adaptive neuro-fuzzy inference system (ANFIS), have been applied to carbonation depth forecasting with high prediction precision [9–11]. However, the accuracy of these models depends on the quality of the input data. Principal component analysis (PCA), a popular algorithm for solving multicollinearity problems, can optimize artificial neural network models by eliminating redundant data.

This paper presents a novel approach, the PCA–ANFIS model, for predicting carbonation depth in concrete structures. The model combines PCA with ANFIS to eliminate redundant data and optimize the input variables. The practical engineering example presented in this paper demonstrates the superior performance of the proposed PCA–ANFIS model.

## 2. Methods

### *2.1. Principal Component Analysis (PCA)*

In practical applications, researchers are often faced with datasets containing multiple correlated indicators. This correlation makes the analysis of these datasets more complex and difficult. Principal component analysis (PCA) is a statistical method that can be used to address this problem by reducing the dimensionality of the data.

PCA involves the linear transformation of high-dimensional datasets into a smaller number of comprehensive indicators, which are known as principal components. These principal components are ranked according to the variance that they explain in the data [12,13]. The principal component with a larger variance contains more information and contributes more to explaining the variability in the data. This makes PCA a useful tool for identifying the most important variables in a dataset and reducing the dimensionality of the data to enhance analysis.

#### 2.1.1. The Basic Idea and Theoretical Foundation of Principal Component Analysis

Principal component analysis (PCA) is a useful technique for reducing the number of dimensions in a dataset prior to modeling. Mathematically, PCA combines original multiple indices into a linear combination of variables. $F_i = a_{1i}X_1 + a_{2i}X_2 + \cdots + a_{Pi}X_P$. Without any restrictions, there could be many linear combinations. Hence, there are specific requirements placed on this linear combination to ensure that it is useful [14–16].

(1) $F_1, F_2, \cdots, F_p$ reflects the information for the original indexes. This is determined by the values of variance sorted in descending order. The greater the variance explained by a principal component, the more information it contains from the original indices. $F_1$ is

called the first principal component, $F_2$ is called the second principal component, and $F_{\mathrm{i}}$ is called the ith principal component.

(2) The second requirement for PCA linear combination is that each principal component should exclude the information contained in the preceding principal components. This means that the principal components should be independent of each other, ensuring that subsequent components do not contain information from previous ones.

2.1.2. Principal Component Analysis of Carbonation Depth

To apply PCA to the carbonation depth prediction model, six influential factors were selected: the compressive strength of the concrete, service life, carbon dioxide concentration, working stress, temperature, and humidity. The following steps were taken for PCA:

(1) The first step in PCA involved standardizing the correlative matrix of the dataset from the input variables to many samples. The coefficient matrix was then calculated, and the secular equation was derived from it; finally, the eigenvalues $\lambda_i$($i$ = 1, 2, ..., 6) and eigenvectors of the correlation matrix were obtained.

(2) The variance contribution proportion VCP ($\beta_i$) was calculated according to the eigenvalues ($\lambda_i$) of the covariance matrix, and the contribution of cumulative variance proportion CVCP ($\eta_i$) was calculated from the cumulative sum of the variance contribution proportion. VCP ($\beta_i$) and CVCP ($\eta_i$) can be calculated using the following equations:

$$\beta_i = \frac{\lambda_i}{\sum\limits_{j=1}^{p} \lambda_i} \tag{1}$$

$$\eta_i = \frac{\sum\limits_{k=1}^{i} \lambda_k}{\sum\limits_{k=1}^{p} \lambda_k} \tag{2}$$

where $\beta_i$ is the variance contribution proportion and $\eta_i$ is the cumulative variance contribution proportion.

(3) The third step of PCA involved identifying the principal components. This is typically accomplished by checking whether the cumulative value of the component variance percentage (CVCP) satisfies a specific standard or whether the eigenvalue is above 70–80% [17]. Once the principal components are identified, a matrix composed of the corresponding eigenvectors of the eigenvalues of every principal component is generated. This matrix is referred to as the component projection matrix or score coefficient matrix. The original dataset can then be converted into a reduced-dimension sample matrix and projected using this projection matrix.

(4) The correlation coefficient was calculated between the sequences as follows:

$$F_i = \alpha_{1i} X_1 + \alpha_{2i} X_2 + \ldots + \alpha_{Pi} X_P \tag{3}$$

where $F_i$ is the principal component and $\alpha_i = (\alpha_{1i}, \alpha_{2i}, \cdots, \alpha_{pi})$ is the relational degrees of the principal component with the initial variables.

The relational coefficient is $\sqrt{\lambda_i}\alpha_{ji}$ between the principal component and $X_j$ variables; the coefficients in Equation (1) should satisfy ${\alpha_{1i}}^2 + {\alpha_{2i}}^2 + \cdots + {\alpha_{pi}}^2 = 1$, $i = 1, 2, \cdots, p$.

*2.2. Adaptive Neuro-Fuzzy Inference System (ANFIS)*

The fuzzy neural network is a combination of neural networks and fuzzy logic, which offers the advantages of both linear and non-linear processes [18]. The neural network is composed of a set of connected artificial neurons using computational connection methods to process information [19]. The adaptive neural network (ANN) can understand the relationships between the data input and output when it has sufficient information [20]. The calculation principles and methods of ANN can be found in the literature [21]. Recently, neural networks and fuzzy logic systems have garnered significant attention in the field of intelligent control, as they can adjust inputs and outputs through a hybrid algorithm that combines back-propagation learning methods with the least squares method. The hybrid algorithm can also automatically generate if–then rules while allowing the fuzzy logic system to adapt membership function parameters. This enables the relevant FIS to detect and trace the given input and output data [22,23].

The nonlinear mapping ability of neural networks allows for massive information storage, error tolerance, self-adaptive learning, and the ability to store incorrect information. These capabilities drive the ANFIS system toward self-adaptation, self-organization, and self-learning, making intelligence, self-adaptation, and optimization the primary development trend of ANFIS.

The ANFIS model is composed of five layers, with each layer consisting of several nodes. Similar to neural networks, the inputs of each layer are obtained by the nodes from the previous layer in the ANFIS structure. Figure 1 describes an ANFIS structure. Figure 1 shows that the neural network contains $m$ inputs $(X_1, X_2, \ldots X_m)$, each one comprising $n$ MFs; in addition, a layer with R fuzzy rules and an output layer contributed to the construction of the model. In the first layer, the number of nodes can be calculated by $N = m \times n$. The number of nodes in other layers (layers 2–4) is related to the number of fuzzy rules (R) [24,25].

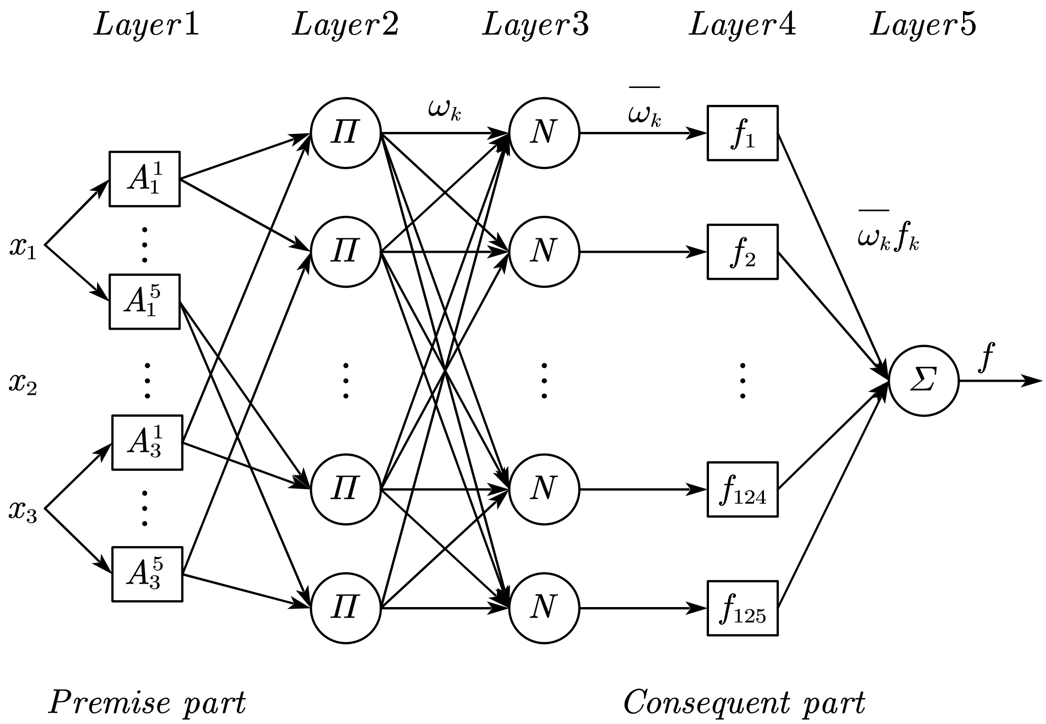


**Figure 1.** The structure of the ANFIS model.

Each layer in an ANFIS model is described as follows:

The boxes in the figure mean that the relevant parameter can be adjusted adaptively at each node, and the circle is the opposite. The first layer is the fuzzy layer; input data are fuzzed in this layer and input data are converted to linguistic type $A_{ij}$ using membership functions. The output of the first layer is as follows:

$$O_{ij}^1 = \mu_{ij}(X_i), i = 1, 2, \ldots, m, j = 1, 2, \ldots n \quad (4)$$

where $\mu_{ij}$ is the $j$th MF for input $X_i$.

The second layer is the product layer. The output of each node represents the excitation intensity of a fuzzy rule, and each node can be gained by multiplying the linguistic inputs calculated in the first layer:

$$O_k^2 = W_k = \mu_{1e_1}(X_1)\mu_{2e_2}(X_2)\ldots\mu_{me_m}(X_m) \tag{5}$$

where $k = 1, 2, \ldots, R$ and $e_1, e_2, \ldots, e_m = 1, 2, \ldots n$.

The third layer is the normalized layer: the ratio of the incentive intensity of the jth fuzzy rule to the sum of the incentive intensities of all rules:

$$O_k^3 = \overline{W}_k = \frac{W_k}{W_1 + W_2 + \ldots + W_k} \tag{6}$$

The fourth layer is the defuzzification layer; each node of this layer is an adaptive node with node function, and the weighted output of each node depends on the if–then rules. The output of the fourth layer is as follows:

$$O_k^4 = \overline{W}_k f_k \tag{7}$$

where $f_k$ represents the output of $k$th fuzzy rules. The rules are expressed as follows:

If ($X_1$ is $A_{1e_1}$) and ($X_2$ is $A_{2e_2}$) and ... and ($X_m$ is $A_{me_m}$), then:

$$f_k = \sum_{1=1}^{m} p_{ie_1} X_i + r_k \tag{8}$$

where $p_{ie_i}$ and $r_k$ are the consequent parameters, $e_1, e_2, \ldots, e_m = 1, 2, \ldots n$, and $k = 1, 2, \ldots, R$.

The fifth layer is the output layer:

$$O_k^5 = Y = \sum_{K=1}^{n} \overline{W}_k f_k \tag{9}$$

In this study, the root mean square error (RMSE) was selected for the inspection of training and checking model performances; it is expressed by the following equation:

$$RMSE = \sqrt{\frac{\sum_{Z=1}^{M}(S_Z - Y_Z)^2}{M}} \tag{10}$$

where $M$ is the total number of training factors, $S_Z$ is the measured data, and $Y_Z$ is the result from the predictive models.

### 2.3. Adaptive Data

To demonstrate the practicality and validity of the PCA–ANFIS model, fifty groups of measured carbonation data from more places, which had great randomicity due to many factors, were collected. The measured data had great uncertainty or discreteness, leading to relatively large errors in the calculation results of the model. The measured carbonation data are shown in Table 1.

This paper used three models, ANFIS, ANN, and PCA–ANFIS, with 50 datasets to predict the carbonation depth of the concrete structure. For modeling, the carbonation depth data were randomly divided into two groups; 90% (45 data sets) of the carbonation depth data was used for training, and 10% (5 data sets) was used for testing the models. MATLAB software was employed to train the data.

**Table 1.** Carbonation depth data of engineering.

| **NO.** | **1** | **2** | **3** | **4** | **5** | **6** | **7** | **8** | **9** | **10** | **11** | **12** | **13** |
|---|---|---|---|---|---|---|---|---|---|---|---|---|---|
| y/a | 5 | 5 | 5 | 5 | 5 | 5 | 5 | 3 | 15 | 15 | 39 | 39 | 13 |
| $f_c$/MPa | 20 | 20 | 20 | 20 | 20 | 25 | 20 | 20 | 28 | 28 | 28 | 38 | 28 |
| T/°C | 21.3 | 21.3 | 21.3 | 21.3 | 21 | 21 | 21 | 13.3 | 18.3 | 18.3 | 11.6 | 11.6 | 15.4 |
| H | 0.8 | 0.8 | 0.8 | 0.8 | 0.8 | 0.8 | 0.8 | 0.71 | 0.8 | 0.8 | 0.59 | 0.59 | 0.77 |
| $kco_2$ | 1.5 | 1.5 | 2 | 2 | 1.8 | 1.8 | 1.8 | 2 | 1.8 | 1.8 | 1.8 | 1.8 | 1.4 |
| $k_s$ | 1.1 | 1 | 1.1 | 1 | 1.1 | 1 | 1 | 1.1 | 1 | 1.1 | 1 | 1 | 1 |
| X/mm | 12 | 10 | 14 | 16 | 12 | 10 | 10 | 17.2 | 8.8 | 8.85 | 20.5 | 15 | 10 |
| NO. | 14 | 15 | 16 | 17 | 18 | 19 | 20 | 21 | 22 | 23 | 24 | 25 | 26 |
| y/a | 52 | 52 | 32 | 56 | 56 | 18 | 18 | 12 | 12 | 35 | 31 | 31 | 31 |
| $f_c$/MPa | 18 | 18 | 28 | 18 | 18 | 28 | 38 | 28 | 28 | 10 | 18 | 28 | 18 |
| T/°C | 7 | 7 | 9.3 | 15.7 | 15.7 | 15.7 | 15.7 | 15.7 | 15.7 | 13.3 | 13.3 | 13.3 | 13.3 |
| H | 0.65 | 0.65 | 0.6 | 0.8 | 0.8 | 0.8 | 0.8 | 0.8 | 0.8 | 0.71 | 0.71 | 0.71 | 0.71 |
| $kco_2$ | 1.4 | 1.4 | 1.2 | 1.2 | 1.2 | 1.2 | 1.2 | 1.2 | 1.2 | 1.2 | 1.4 | 1.4 | 1.2 |
| $k_s$ | 1 | 1.1 | 1 | 1 | 1.1 | 1 | 1.1 | 1 | 1 | 1 | 1 | 1.1 | 1 |
| X/mm | 45 | 38 | 7 | 25 | 20 | 8.5 | 10 | 5.95 | 8.7 | 23.2 | 12.8 | 11.1 | 24 |
| NO. | 27 | 28 | 29 | 30 | 31 | 32 | 33 | 34 | 35 | 36 | 37 | 38 | 39 |
| y/a | 31 | 31 | 40 | 40 | 21 | 32 | 32 | 32 | 4 | 30 | 30 | 30 | 30 |
| $f_c$/MPa | 28 | 28 | 28 | 28 | 28 | 25 | 20 | 15 | 30 | 38 | 20 | 20 | 25 |
| T/°C | 13.3 | 13.3 | 7.3 | 7.3 | 7.3 | 7.3 | 7.3 | 7.3 | 13.3 | 13.3 | 13.3 | 13.3 | 13.3 |
| H | 0.71 | 0.71 | 0.57 | 0.57 | 0.57 | 0.46 | 0.46 | 0.46 | 0.71 | 0.71 | 0.71 | 0.71 | 0.71 |
| $kco_2$ | 1.2 | 1.2 | 1.4 | 1.4 | 1.4 | 1.2 | 1.2 | 1.2 | 1.4 | 1.2 | 1.2 | 1.2 | 1.2 |
| $k_s$ | 1 | 1.1 | 1 | 1 | 1 | 1.1 | 1.1 | 1 | 1.1 | 1 | 1 | 1 | 1 |
| X/mm | 15 | 26 | 10.8 | 10.1 | 6.2 | 15 | 19 | 23 | 5.22 | 11.4 | 20.1 | 20.4 | 21.3 |
| NO. | 40 | 41 | 42 | 43 | 44 | 45 | 46 | 47 | 48 | 49 | 50 | | |
| y/a | 16 | 13 | 16 | 26 | 26 | 22 | 22 | 31 | 40 | 38 | 40 | | |
| $f_c$/MPa | 18 | 18 | 18 | 18 | 28 | 18 | 18 | 20 | 18 | 18 | 18 | | |
| T/°C | 13 | 13 | 13 | 1.14 | 1.14 | 16.3 | 16.3 | 16.3 | 16.3 | 16.3 | 16.3 | | |
| H | 0.65 | 0.65 | 0.65 | 0.59 | 0.59 | 0.79 | 0.79 | 0.79 | 0.79 | 0.79 | 0.79 | | |
| $kco_2$ | 1.4 | 1.4 | 1.4 | 1.2 | 1.2 | 1.4 | 1.4 | 1.2 | 1.2 | 1.2 | 1.2 | | |
| $k_s$ | 1 | 1 | 1 | 1 | 1 | 1 | 1 | 1.1 | 1 | 1 | 1 | | |
| X/mm | 32.4 | 12.2 | 19.5 | 6.4 | 7.5 | 31.8 | 37.6 | 24 | 28.15 | 17.3 | 15.4 | | |

## 3. Analysis of the Practical Engineering Data and Results

The practical engineering data used in this study are listed in Table 1 and were sourced from previous literature [3] that focused on carbonation depth forecasting in concrete structures. The data were used to verify the superiority of the proposed PCA–ANFIS model. Carbonation depth is influenced by many factors, including the compressive strength of the concrete, service life, carbonation time, impact factors of carbon dioxide emission in the air, impact factors of the stress state of the concrete structure, temperature, and humidity.

Due to the highly nonlinear relationship between carbonation depth and other influencing factors, the principal component analysis method was used to reduce the dimensions of the original input data; the reduced variables were used as the input data of the adaptive neural fuzzy inference system; and the results were obtained after iterative calculation. Finally, the prediction model of carbonation depth based on the PCA–ANFIS network was established.

### 3.1. Principal Component Analysis for Concrete Cover Crack

In Table 1, the carbonation depth h is considered the output sequence, compressive strength of concrete $f_c$/MPa; the service life y/a, the impact factor of carbon dioxide concentration $k_{co_2}$, the impact factor of working stress of the concrete structure $k_s$, temperature T/°C, and humidity H serve as the influence sequence.

The principal component analysis of all influencing factors was carried out, as shown in Table 2. The principal component selection criteria were that the CVCP exceeded 70–80%. Since the CVCP of the first through the fourth principal components represented approximately 90.23%, these four components already contained most of the message required for the evaluation. This shrunk the model scale because the first six influential factors were reduced to four. According to Equation (3), the high-dimensional input matrix with six variables in Table 1 was transformed into a low-dimensional one with four variables. The PCA results are shown in Table 3.

**Table 2.** Analysis results of PCA.

| Principal Component No. | Eigenvalues $\lambda_i$ | VCP | CVCP (%) |
|---|---|---|---|
| 1 | 2.28 | 41.31 | 41.31 |
| 2 | 1.29 | 19.71 | 61.02 |
| 3 | 0.99 | 15.40 | 76.42 |
| 4 | 0.88 | 13.81 | 90.23 |
| 5 | 0.46 | 7.82 | 98.05 |
| 6 | 0.11 | 1.95 | 100.00 |

**Table 3.** Summary of data after dimension reduction by the PCA method.

| NO. | 1 | 2 | 3 | 4 | 5 | 6 | 7 | 8 | 9 | 10 | 11 | 12 | 13 |
|---|---|---|---|---|---|---|---|---|---|---|---|---|---|
| Y1 | 2.41 | 2.10 | 3.23 | 2.92 | 2.87 | 2.56 | 2.55 | 1.90 | 1.92 | 2.23 | −0.69 | −0.69 | 0.83 |
| Y2 | 0.15 | −0.84 | 0.78 | −0.21 | 0.54 | 0.10 | −0.45 | 1.52 | 0.39 | 1.38 | 1.05 | 2.15 | 0.17 |
| Y3 | −1.28 | 0.60 | −1.19 | 0.69 | −1.23 | 1.04 | 0.65 | −1.16 | 1.14 | −0.74 | 0.77 | 1.54 | 1.10 |
| Y4 | 0.16 | −0.31 | −0.96 | −1.43 | −0.53 | −0.54 | −0.99 | −1.72 | −0.18 | 0.29 | −0.92 | −0.02 | 0.43 |
| NO. | 14 | 15 | 16 | 17 | 18 | 19 | 20 | 21 | 22 | 23 | 24 | 25 | 26 |
| Y1 | −2.02 | −1.70 | −1.67 | −0.70 | −0.39 | 0.53 | 0.84 | 0.72 | 0.72 | −0.76 | −0.30 | 0.02 | −0.63 |
| Y2 | −0.78 | 0.21 | 0.49 | −2.05 | −1.06 | −0.29 | 1.80 | −0.19 | −0.19 | −2.13 | −0.93 | 1.16 | −1.18 |
| Y3 | −0.25 | −2.13 | 0.77 | −0.34 | −2.22 | 0.99 | −0.11 | 1.08 | 1.08 | −0.67 | 0.05 | −1.05 | 0.01 |
| Y4 | −0.58 | −0.12 | 0.24 | 0.96 | 1.43 | 1.12 | 2.49 | 1.00 | 1.00 | −0.68 | −0.48 | 0.89 | −0.03 |
| NO. | 27 | 28 | 29 | 30 | 31 | 32 | 33 | 34 | 35 | 36 | 37 | 38 | 39 |
| Y1 | −0.62 | −0.31 | −1.99 | −1.99 | −1.37 | −2.29 | −2.29 | −2.61 | 0.89 | −0.59 | −0.59 | −0.59 | −0.59 |
| Y2 | −0.08 | 0.91 | 0.81 | 0.81 | 1.13 | 1.75 | 1.20 | −0.34 | 1.85 | 1.04 | −0.94 | −0.94 | −0.39 |
| Y3 | 0.79 | −1.09 | 0.69 | 0.69 | 0.96 | −1.37 | −1.76 | −0.27 | −0.50 | 1.59 | 0.18 | 0.18 | 0.57 |
| Y4 | 0.87 | 1.34 | −0.27 | −0.27 | −0.64 | −0.28 | −0.73 | −1.65 | 0.54 | 1.76 | 0.13 | 0.13 | 0.58 |
| NO. | 40 | 41 | 42 | 43 | 44 | 45 | 46 | 47 | 48 | 49 | 50 | | |
| Y1 | −0.15 | −0.05 | −0.15 | −2.50 | −2.49 | 0.74 | 0.74 | 0.44 | −0.17 | −0.10 | −0.17 | | |
| Y2 | −0.44 | −0.39 | −0.44 | −0.09 | 1.01 | −1.20 | −1.20 | −0.40 | −1.76 | −1.73 | −1.76 | | |
| Y3 | 0.26 | 0.30 | 0.26 | 0.10 | 0.88 | 0.19 | 0.19 | −1.70 | −0.11 | −0.08 | −0.11 | | |
| Y4 | −1.06 | −1.12 | −1.06 | −1.15 | −0.25 | −0.17 | −0.17 | 1.10 | 0.63 | 0.59 | 0.63 | | |

### *3.2. Establishment of Predicting Models Based on ANFIS, ANN, PCA–ANN, and PCA–ANFIS Models*

Using practical engineering data on carbonation depth in concrete structures from Table 1, this study employed principal component analysis (PCA) to establish the traditional ANFIS model, the ANN model, the PCA–ANN model, and the PCA–ANFIS model for carbonation depth forecasting. The data in Table 3 after dimension reduction by PCA were used as the input vector for the PCA–ANFIS model and the PCA–ANN model, while the data in Table 1 formed the input vector for the ANFIS model and the ANN model, with carbonation depth as the output vector in both cases. For both models, 45 subsamples were retained as training data, with the remaining five subsamples used as checking data.

The predicted results were influenced by the parameter set for the ANFIS models and PCA–ANFIS models, including the type of fuzzy-based rule, the number of membership functions (MFs), and the membership function types [26]. For the ANFIS model and the

ANN model, six nodes were used in the input layer, and one node was used in the output layer. By contrast, the PCA–ANFIS and PCA–ANN models had four nodes in the input layer and one node in the output layer according to the results of PCA. After conducting multiple fitting trials, the RMSE value was set to $6.5 \times 10^{-4}$, the iteration number was set to 136 epochs, and the structures with different MFs for each input 2-2-4-3 topography were found to have the lowest values of RMSE. The choice of membership functions also influenced the accuracy results, with the generalized bell being selected to train and check the network based on its testing performances.

Overall, this study aimed to improve the accuracy of carbonation depth forecasting in concrete structures by using PCA and ANFIS models to reduce the dimensionality of the input data and test the combination of these models.

### 3.3. Comparison of Calculation Results

The model structure with 2-2-4-3 for the PCA–ANFIS model with four nodes is shown in Figure 2; the membership function plots of gbellmf of the four inputs were all the same, and the Levenberg–Marquardt algorithm of ANN was selected. Table 4 shows the RMSE of the ANFIS, ANN, PCA–ANN, and PCA–ANFIS models, and Table 5 shows the measured values and predicted values by the ANN, ANFIS, PCA–ANN, and PCA–ANFIS models. The RMSE of training and checking the results of the above models is shown in Table 5.

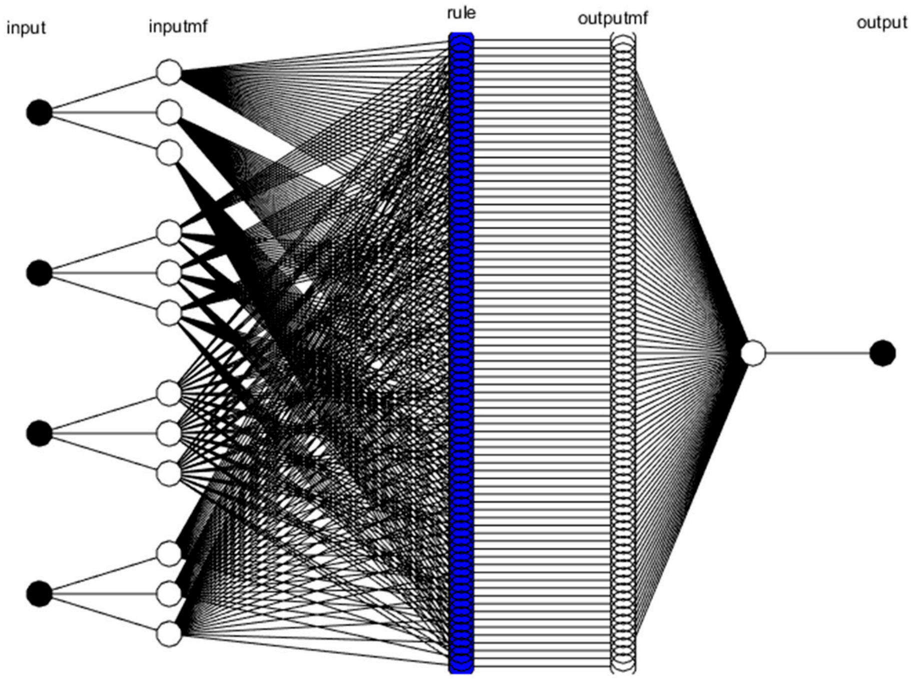


**Figure 2.** The model structure with 2-2-4-3 for the PCA–ANFIS model.

**Table 4.** RMSE of ANFIS, ANN, and PCA–ANFIS models.

| Predicting Model | Type of Membership Functions | Number of MFs | Epochs (Run Times) | Algorithm | RMSE of Checking |
|---|---|---|---|---|---|
| ANN<br>PCA–ANN | | | | Levenberg-<br>Marquardt | 6.28<br>5.42 |
| ANFIS | gbellmf | 3-3-3-3-3-3 | 50 (>20 min) | | 12.23 |
| PCA–ANFIS | gbellmf | 2-2-4-3 | 136 (<30 s) | | 1.38 |

**Table 5.** The results of different models for estimating carbonation depth data for checking data.

| Measuring Data of Carbonation Depth/(mm) | Predicting Value of Carbonation Depth/(mm) by Different Models | | | |
|---|---|---|---|---|
| | ANN | ANFIS | PCA–ANN | PCA–ANFIS |
| 12 | 9.58 | 10.23 | 8.23 | 11.81 |
| 10 | 7.27 | 32 | 21.9 | 8.72 |
| 14 | 7.89 | 21.56 | 13.1 | 14.26 |
| 16 | 6.31 | 3.27 | 21.46 | 15.63 |
| 12 | 13.67 | 18.46 | 8.67 | 9.2 |

## 4. Discussion

As shown in Table 4, both the ANFIS and PCA–ANFIS models employed gbellmf membership functions, with the number of MFs set to three for each input, 3-3-3-3-3-3 topography for ANFIS, and 2-2-4-3 topography for PCA–ANFIS. The PCA–ANFIS model demonstrated higher efficiency due to PCA's dimensionality reduction, resulting in faster convergence times than the ANFIS model, which had redundant inputting variables, as evidenced by the time taken to run 50 epochs. In addition, Table 4 shows that the PCA–ANFIS model achieved higher performance accuracy than the ANFIS and ANN models.

Because the carbonation depth data was collected from actual engineering, the prediction accuracy was likely affected by different criteria in data collection and calculation methods.

The combined model PCA–ANFIS has strong learning and expression abilities, but the selection of fuzzy rule conclusion parameters and membership function parameters is a key factor hindering the improvement of ANFIS performance, which limits the application and forecast accuracy of the ANFIS model. Therefore, it requires optimization algorithms to enhance the ANFIS conclusion parameters and membership function parameters to obtain higher forecast accuracy for carbonation depth.

## 5. Conclusions

The carbonation depth of concrete is a vital parameter for evaluating the durability of reinforced concrete structures. The factors influencing concrete carbonation depth are complex and unpredictable, including concrete compressive strength, service life, carbonation time, carbon dioxide concentration, working stress, temperature, and humidity. In this paper, the ANFIS and PCA–ANFIS models were used to predict the carbonation depth of concrete, and the following conclusions were drawn:

(1) Principal component analysis (PCA) effectively resolved the multicollinearity issue between the original inputs of the neural network, resulting in a reduction in the number of inputs for the neural network. This ensured the neural network's prediction accuracy while reducing its training time.

(2) Comparing the RMSE of the ANFIS, ANN, PCA–ANN, and PCA–ANFIS models showed that the forecasting accuracy of the PCA–ANFIS model was higher than that of the ANFIS model, and that of the PCA–ANN model was higher than that of the ANN model; in addition, the model's running time was saved. This demonstrated that the PCA–ANFIS model can provide reliable and scientific guidance for predicting the carbonation depth of concrete structures.

(3) The carbonation of concrete is influenced by various factors with complex relationships, especially when practical engineering data are hard to obtain. The Bayesian network's advantage is evident. The use of the PCA–ANFIS model can effectively predict the carbonation depth of concrete structures in similar situations.

**Author Contributions:** X.B.: implementation of the computer code and supporting algorithms; J.L.: providing ideas and conducting writing, review, and editing. All authors have read and agreed to the published version of the manuscript.

**Funding:** This research was funded by the Liaoning Provincial Education Department, Grant LJKZ0425, China, and by Liaoning Petrochemical University, Grant No. 1100130241.

**Institutional Review Board Statement:** Not applicable.

**Informed Consent Statement:** Not applicable.

**Data Availability Statement:** The carbonation depth data used to support the findings of this study are included in the book 'Durability and Life Forecast of Reinforced Concrete Structure'.

**Acknowledgments:** We would like to thank Yan, Z.Y. for designing computer programs and conducting data processing; Tong, H.Y. for conducting the presentation of the published work; and Zhang, F.Y. for the validation of the proposed model and language improvement.

**Conflicts of Interest:** The authors declare no conflict of interest.

## References

1. Xiao, J.; Gou, C.F. Overview of the research for concrete carbonation. *Concrete* **2010**, *1*, 40–44.
2. Jin, Z.Q.; Sun, W.; Zhang, Y.S.; Liu, Z.Y. Study on Carbonation of Concrete under Loading. *J. Mater. Eng.* **2005**, *8*, 179–183.
3. Niu, D.T. Concrete Carbonation and Forecasting Model. In *Durability and Life Forecast of Reinforced Concrete Structures*, 1st ed.; Tong, A.Q., Liu, B.L., Eds.; Science Press: Beijing, China, 2003; pp. 10–23.
4. Khunthongkeaw, J.; Tangtermsirikul, S.; Leelawat, T. A study on carbonation depth prediction for fly ash concrete. *Constr. Build. Mater.* **2016**, *20*, 744–753. [CrossRef]
5. Yamada, T.; Kikuchi, M.; Saito, T.; Saeki, T. Prediction of carbonation progress using mortar thin plate specimen. *Cem. Sci. Concr. Technol.* **2013**, *67*, 370–377. [CrossRef]
6. Wojciechowski, P.P.; Sokolowska, J.J. Self-terminated carbonation model as a useful support for durable concrete structure designing. *Struct. Eng. Mech.* **2017**, *63*, 55–64.
7. Wu, R.; Liu, J.; Zhang, G.; Zhang, Y.; An, S. Research on Carbonation Characteristics and Frost Resistance of Iron Tailings Powder Concrete under Low-Cement Clinker System. *Adv. Mater. Sci. Eng.* **2020**, *2020*, 9192757. [CrossRef]
8. Sharma, P.; Said, Z.; Kumar, A.; Nižetić, S.; Pandey, A.; Hoang, A.T.; Huang, Z.; Afzal, A.; Li, C.; Le, A.T.; et al. Recent Advances in Machine Learning Research for Nanofluid-Based Heat Transfer in Renewable Energy System. *Energy Fuel* **2022**, *36*, 6626–6658. [CrossRef]
9. Luo, D.; Niu, D.; Dong, Z. Application of Neural Network for Concrete Carbonation Depth Prediction. *Int. J. Concr. Struct M* **2014**, *7*, 24–26.
10. Akpınar, P.I.; Uwanuakwa, D. Intelligent prediction of concrete carbonation depth using neural networks. *Bull. Transilv. Univ. Bras. Ser. III Math. Inf. Phys.* **2016**, *9*, 99–107.
11. Wang, X.L.; Tong, T.H.; Zhang, H.M. A prediction model for concrete carbonation based on ANFIS. *NEFU* **2006**, *4*, 76–77+113.
12. Peng, Z.Y.; Liu, W.S. Principal Component Analysis of Long-Lag, Wide-Pulse Gamma-Ray Burst Data. *J. Astrophys. Astron.* **2014**, *35*, 527–528. [CrossRef]
13. Chen, C.; He, X.; Guo, B.; Zhao, X.; Chu, Y. A pixel-level fusion method for multi-source optical remote sensing image combining the principal component analysis and curvelet transform. *Earth Sci. Inform.* **2020**, *13*, 1005–1013. [CrossRef]
14. Gao, W.; Han, J. Prediction of destroyed floor depth based on principal component analysis (PCA)-genetic algorithm (ga)-support vector regression (SVR). *Geotech. Eng.* **2020**, *38*, 3481–3491. [CrossRef]
15. Gauri, S.K.; Pal, S. The principal component analysis (PCA)-based approaches for multi-response optimization: Some areas of concerns. *Int. J. Adv. Manuf. Tech.* **2014**, *70*, 1875–1887. [CrossRef]
16. Liu, B.; Liang, B. Prediction of seam floor water inrush based on combining principal component analysis and support vector regression. *Coal Geol. Explor.* **2011**, *39*, 29–35.
17. Zhu, H.; Zhu, B. Principal Component Analysis, Factor Analysis, and Correspondence Analysis. In *Application Statistics and SPSS Application*; Yang, L.J., Ed.; Publishing House of Electronics Industry: Beijing, China, 2011; pp. 665–668.
18. Pratama, M.; Rajab, S.; Joo, E. Extended Approach of ANFIS in Cascade Control. *Int. J. Comput. Electr. Eng.* **2011**, *3*, 1–5. [CrossRef]
19. Khan, I.H.; Sablani, S.S.; Joardder, M.U.H.; Karim, M.A. Application of machine learning-based approach in food drying: Opportunities and challenges. *Dry. Technol.* **2020**, *40*, 1051–1067. [CrossRef]
20. Aghbashlo, M.; Hosseinpour, S.; Mujumdar, A.S. Application of Artificial Neural Networks (ANNs) in Drying Technology: A Comprehensive Review. *Dry. Technol.* **2015**, *33*, 1397–1462. [CrossRef]
21. Sharabiani, V.R.; Kaveh, M.; Taghinezhad, E.; Abbaszadeh, R.; Khalife, E.; Szymanek, M.; Dziwulska-Hunek, A. Application of Artificial Neural Networks, Support Vector, Adaptive Neuro-Fuzzy Inference Systems for the Moisture Ratio of Parboiled Hulls. *Appl. Sci.* **2022**, *12*, 1711. [CrossRef]
22. Kariminia, S.; Motamedi, S.; Shamshirband, S.; Petkovic, D.; Roy, C.; Hashim, R. Adaptation of anfis model to assess thermal comfort of an urban square in a moderate and dry climate. *Stoch. Environ. Res. Risk Access.* **2016**, *30*, 1189–1203. [CrossRef]
23. Mousavi, J.; Ponnambalam, K.; Karray, F. Inferring operating rules for reservoir operations using fuzzy regression and ANFIS. *Fuzzy Set. Syst.* **2007**, *158*, 1064–1082. [CrossRef]

24. Patel, D.; Parekh, F. Flood Forecasting using Adaptive Neuro-Fuzzy Inference System. *Int. J. Eng. Sci.* **2014**, *12*, 510–514.
25. Gite, A.V.; Bodade, R.M.; Raut, B.M. ANFIS Controller and its Application. *ESRSA Publ.* **2013**, *2*, 1–5.
26. Mashallah, R.; Amir, D.; Morteza, A. H 2-selective mixed matrix membranes modeling using ANFIS, PSO-ANFIS, GA-ANFIS. *Int. J. Eng. Sci.* **2017**, *42*, 15211–15225.